

Transition from reflection to sticking in ultracold atom-surface scattering

Areez Mody, John Doyle and Eric J. Heller

Department of Physics, Harvard University, Cambridge, MA 02138

(August 2000)

In paper I [1] we showed that under very general circumstances, atoms approaching a surface will not stick as its incoming energy approaches zero. This is true of either warm or cold surfaces. Here we explore the transition region from non sticking to sticking as energy is increased. The key to understanding the transition region is the WKB approximation and the nature of its breakdown. Simple rules for understanding the rollover to higher energy, post-threshold behavior, including analytical formulae for some asymptotic forms of the attractive potential are presented. We discuss a practical example of atom-surface pair in various substrate geometries. We also discuss the case of low energy scattering from clusters.

I. INTRODUCTION

The problem of sticking of atoms to surfaces at very low collision velocities has a long history and has met with some controversy. The issue goes back to the early distorted wave Born approximation results of Lennard-Jones [3], who obtained the threshold law sticking probability going as k in the limit of low velocities. This paper is a companion to paper I [1], wherein we put the problem on a firmer theoretical foundation. We showed (non-perturbatively) that in an ultracold collision a simplistic one-body view of things is essentially correct even if the number of internal degrees of freedom is very large. We concluded that approaching atoms will not stick to surfaces if the approach velocity is low enough, even if the surface is warm. From the methods used, it is clear that the non-sticking rule would apply to clusters as well as semi-infinite surfaces, and would also apply to projectiles more complex than atoms.

From an experimental perspective atom-surface sticking could impact the area of guiding and trapping atoms in material wires and containers. In those applications it is necessary to predict the velocities needed for quantum reflection, sticking, and the transition regime between them. We do so in this paper.

Above a certain temperature or kinetic energy, but still well below the attractive well depth of the atom surface potential, atoms will stick to surfaces with near 100 percent certainty. The reason for this is simple: Classical trajectory simulations of atom-surface collisions at low collision velocities indicate sticking with near certainty because the acceleration in the attractive regime is followed by a hard collision with the wall. This almost always leads to sufficient energy loss from the particle to the surface that immediate escape is not possible. This

is true so long as the approach energy is significantly less than the well depth, which is itself greater than the temperature of the surface. Therefore, the onset of quantum reflection is heralded by a break down in the WKB approximation - an approximation based purely on the (sticking) classical trajectories.

Thus, there must exist a transition region between the non-sticking regime for very low collision velocities, and the sticking regime at higher velocities. The key to understanding the transition region is to understand the validity of classical mechanics (WKB) as applied to the sticking problem. The correctness of the simplistic one-body physics of quantum reflection from the surface, focusses our study on the WKB approximation to the coordinate normal to the surface. The entrance channel wavefunction thus obtained may also be used as input into the Golden Rule to study the threshold behaviour of the inelastic cross-sections. We do this in Section VI. The nonsticking threshold behavior we established in paper I is interpreted as an extension of the validity of the so-called Wigner threshold behavior. We are also able to make definite predictions about the nature of the post threshold behavior of sticking in terms of inelastic cross-sections. (Section VI).

II. QUANTUM REFLECTION AND WKB

We consider the typical case of an attractive potential arising out of the cumulative effect of Van der Waals attractions between target and incident atoms. A classical atom would proceed straight into the interaction region showing no sign of reflection, but the quantum mechanical probability of being found inside is suppressed by a factor of k (as $k \rightarrow 0$) as compared to the classical probability (Section VIA 1), where k is the wave vector of the incoming atom. This is tantamount to saying that quantum mechanically the amplitude is reflected back without penetrating the interaction region, analogous to the elementary case of reflection from the edge of a step-down potential in one dimension while attempting to go over the edge. A useful way to view this is to attribute the reflection to the failure of the WKB approximation.

To be specific, we keep the geometry of paper I in mind: an atom is incident from the right ($x > 0$) upon the face of a slab ($x = 0$) that lies to the left of $x = 0$. For a low incoming energy $\epsilon \equiv \hbar^2 k^2 / 2m$, a left-moving WKB solution begun well inside the interaction region will fail to match onto a purely left-going WKB solution as we integrate out to large distances because the WKB

criterion

$$|\lambda'(x)| = \left| \frac{\hbar p'}{p^2} \right| \ll 1 \quad (1)$$

for the local accuracy of the wavefunction will in general fail to be valid in some intermediate region. For bounded potentials that turn on abruptly for example at $x = a$, it is obvious that WKB will fail near $x \sim a$. For long-range potentials such as a power law $V(x) = -c_n/x^n$ it is not immediately obvious where this region of WKB failure lies, if it exists at all. It turns out that even in this case it is possible to identify (for small enough ϵ) a distance (dependent on ϵ) at which the potential ‘turns on’ and where WKB will fail. We will show below that WKB is at its worst ($|\lambda'(x)|$ is maximized) at a distance x where the kinetic and potential energies are approximately equal, i.e where $|V(x)| \sim \epsilon$. The distance away from the slab at which the particle is turned around - or quantum reflected - is precisely this distance. Furthermore, one may heuristically expect that the greater the failure of WKB, the greater the reflection.

Fig. 1 shows a plot of the error term in Eq. (1) for three different values of the incoming energy of neon on a semi-infinite slab of SiN. The essential points to notice are:

- 1) There is a greater error incurred in attempting to apply the WKB (classical mechanics) approximation to colder atoms than to warmer ones. Consequently, we expect that the slower the atom, the more non-classical its behavior. In particular, slow enough atoms will be ‘quantum reflected’ and will not stick.
- 2) As the incoming velocity is decreased the atom is reflected at distances progressively further and further away from the slab. This is because the interval in x around which the WKB error is large, may be identified as the region from which the atom is reflected.

A useful qualitative rule of thumb obtained in Section III below is that the region of WKB error reaches all the way out to those regions where the potential energy is still roughly the same order of magnitude as the incoming energy (Eq. (5)). This means that as $\epsilon \rightarrow 0$ the error is still large where the potential energy graph looks essentially flat. In fact as $\epsilon \rightarrow 0$ it is easily shown that a plot of the WKB error will show a non-uniform convergence to a polynomial proportional to

$$x^{\frac{n}{2}-1} \quad \text{for all } n > 0 \quad (2)$$

Fig. 1 shows the case for $n = 3$.

III. WKB FAILURE

Differentiating $p^2/2m + V(x) = \epsilon$ w.r.t. x , we have

$$p' = \frac{-mV'}{p} \quad (3)$$

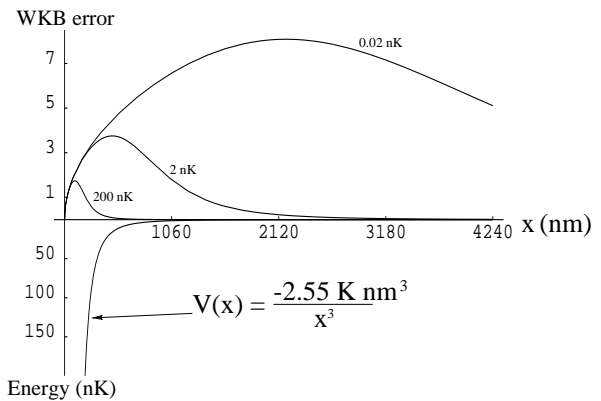


FIG. 1. The WKB error of Eq. (1) for three different values of the incoming energy 200, 2 and 0.02 nK, vs. the distance x nm from the slab (SiN). The long range form of the potential $-c_3/x^3$ ($c_3=220 \text{ meV } \text{\AA}^3$) is also shown for which the negative ‘y-axis’ is calibrated in the different units of energy. The sticking probabilities for the three cases are approximately 1, 0.6, 0.1.

which when used repeatedly to eliminate p' shows that $|p'/p^2|$ in Eq. (1) is maximized when

$$\frac{p^2}{3m} = \frac{V'^2}{V''}. \quad (4)$$

For $V(x) = -c_n/x^n$, this is exactly when

$$|V(x)| = \epsilon \left(\frac{2(n+1)}{n-2} \right). \quad (5)$$

We discover that for $n > 2$ only, we have a point where WKB is at its worst at a distance x where $|V(x)| \sim \epsilon$, and moreover, that this maximum behaves like

$$\max \left| \frac{p'}{p^2} \right| \sim \frac{1}{c_n^{1/n} \epsilon^{\frac{1}{2}-\frac{1}{n}}} \sim \frac{1}{c_n^{1/n} k^{1-\frac{2}{n}}} \quad (6)$$

which for $n > 2$ diverges as $k \rightarrow 0$. Note how a *weaker* potential (smaller c_n) is *better* at reflecting a particle at the same energy, but allows the atom to approach closer. Heuristically a sketch of $V(x) = -c_n/x^n$ reveals why: the weaker potential is seen to turn on more abruptly at a point closer to $x = 0$, promoting a greater breakdown of WKB there. Alternatively a simple scaling argument with Schrodinger’s equation reveals the same trend.

The above conclusions are valid only for $n > 2$. For $n \leq 2$ the error term of Eq. (1) looks qualitatively different from that in Fig. 1. It is small at all distances except near $x = 0$ where it diverges to infinity, as is evident from Eq.(2). If the physical parameters are such that this region where WKB fails very close to the slab is never actually manifest in the long-range part of the potential then the ‘no-reflection’ classical behaviour will be valid all the way up to distances near the slab where the atom will begin to feel the short range forces and loose energy to the internal degrees of freedom. For such

a case then with $n < 2$ we believe one will *not* observe quantum reflection.

IV. STICKING PROBABILITY

Having established that the reflection is caused by a well-defined localized region, we solve the one-dimensional Schrodinger equation around this region to accurately compute the reflection probability. For an attractive power law potential $V(x) = -c_n/x^n$, the relevant one dimensional equation is

$$\left(\frac{d^2}{dx^2} + \frac{a_n^{n-2}}{x^n} + k^2 \right) \phi_e(x) = 0. \quad (7)$$

$\phi_e(x)$ is the entrance channel wavefunction. The length scale

$$a_n \equiv (2mc_n/\hbar^2)^{\frac{1}{n-2}}, \quad (8)$$

contains all the qualitative information about the reflection. Its relevance is twofold. Firstly, the sticking probability for small k , behaves as

$$P_{\text{sticking}} \sim N_n k a_n \quad (9)$$

where N_n is a pure numeric constant (roughly of order 10 for $n = 3$, and of order 1 for $n = 4, 5$), see Ref. [6]. P_{sticking} may be computed numerically for any k , and Fig.2 shows P_{sticking} vs. ka_n for $n = 3, 4$, and 5. Secondly, the distance at which the particle is turned around is estimated by solving

$$\left(\frac{a_n}{x} \right)^n = (ka_n)^2 \quad (10)$$

for x , which is just the requirement that $|V(x)| = \epsilon$. Equation (9) together with equation (8) makes plain that a smaller c_n is more conducive to making quantum reflection happen, while Eq. (10) indicates that the turnaround point is then necessarily closer to the surface. With these effects in mind, we look at some specific cases.

V. EXAMPLES

We examine the case of incidence on a slab which may be treated as semi-infinite, and also the case when it is a thin film. It is useful to first look at these cases pretending there is no Casimir interaction, and assuming that the short range form of the potential is everywhere valid. Afterwards we put in the Casimir interaction. For clarity we will pick a specific example of target and incident atoms for most of our discussions, by specifying the numeric values for the short range potential between the atom and semi-infinite slab, since these are most comprehensively tabulated in reference [4].

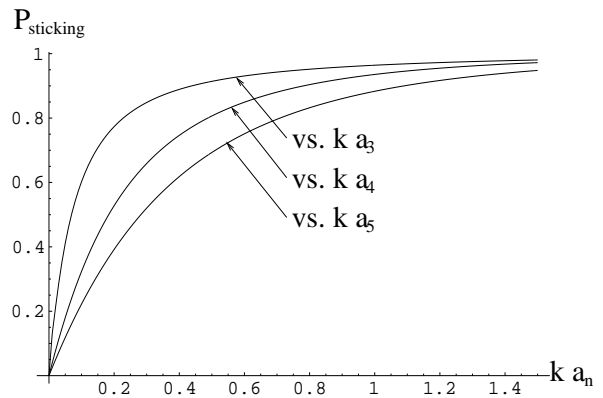


FIG. 2. Sticking probabilities for an atom incident on surface providing a long range interaction of the form $V(x) = -c_n/x^n$ for the cases $n=3,4,5$. Note that the length scale a_n used to compute the dimensionless ka_n coordinate on the ‘x-axis’ vs. which we plot the sticking probabilities, is different for each n .

Fig. 3 shows the sticking probability vs. the temperature of an incoming Ne atom in units of 10^{-9} Kelvin. The slab is silicon-nitride (SiN). The various curves are for the different cases depending on whether we are considering a thick or thin slab, and whether the Casimir effect is included or not. We will discuss these cases below, pointing out the relevant length and energy scales involved in deciding to label the slab as semi-infinite or thin. The mapping from the mathematically natural ka_n (with $n = 3$ and $c_3 = 220 \text{ meV } \text{\AA}^3$) scale of Fig. 2 to the more physical temperature scale of Fig. 3 is made using

$$T \simeq [69.08 \text{ Kelvin}] \left(\frac{m_H}{m_{\text{atom}}} \right)^3 \left(\frac{\text{meV } \text{\AA}^3}{c_3} \right)^2 (ka_3)^2 \quad (11)$$

where we used $\langle \epsilon \rangle = (3/2)k_B T$ to compute the temperature by setting $\langle \epsilon \rangle$ equal to the incoming energy. m_H = mass of hydrogen atom, and for our example $m_{\text{Ne}} = 20.03 m_H$.

All the graphs in Fig. 3 have an initial slope of 0.5 indicating the $\sqrt{\epsilon}$ behaviour of the sticking probabilities once the energies are low enough to be in the Quantum Reflection regime. A particular temperature at which there is a transition to the post-threshold sticking regime, we arbitrarily (but intuitively) define as the temperature where the slope becomes 0.4. For the thin film case of $10 nm$ in our example this temperature is 10 nK.

While the parameters in our example are fairly typical, it is clear that the cubic dependence on mass and quadratic dependence on the c_3 coefficient in Eq.(11), will make this temperature range over quite a few orders of magnitude. The c_3 's in Ref [4], listed in units of $\text{meV} - \text{\AA}^3$ for a variety of surface atom pairs, range in values from 100 to 3000.

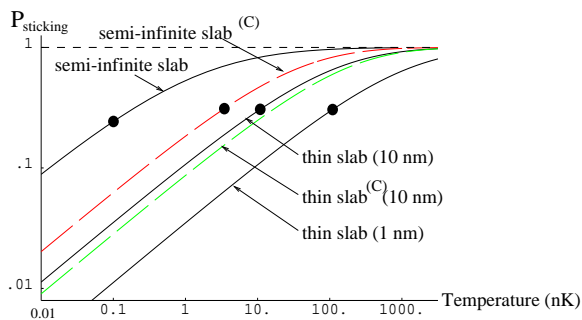


FIG. 3. Sticking probabilities vs temperature of incident Ne atoms on SiN. The broken line indicate the inclusion of the very long range Casimir forces (see text). The large dot demarcates the regions of threshold and post-threshold, using the criterion suggested at the end of Section V

A. Semi-Infinite Slab (without Casimir)

Even though c_3 coefficients are known both theoretically and experimentally for many surface-atom pairs, for completeness we take a moment to look at a quick way of estimating them. This is provided by the London formula

$$V_{\text{atom-atom}}(r) = \frac{-3}{2} \frac{I_A I_B}{I_A + I_B} \frac{\alpha_A \alpha_B}{r^6} \equiv \frac{-c_6}{r^6}, \quad (12)$$

which estimates the Van der Waals interaction between any two atoms. I is the ionization potential and α the polarizability of each atom. Then summing over all the atoms in the semi-infinite slab (thick) we get

$$V_{\text{slab-atom}}(x) = \frac{-\pi c_6 \rho_{\text{atoms}}}{6} \times \frac{1}{x^3} \equiv \frac{-c_3}{x^3} \quad (13)$$

where ρ_{atoms} = the density of slab atoms. These estimates are not very accurate, but correctly indicate the physical quantities on which the answer depends. Reference [4] provides a useful compendium of these coefficients. We have used $c_3 = 220 \pm 4 \text{ meV } \text{\AA}^3$ for neon atoms incident on silicon nitride from work of [5]. This choice of c_3 makes

$$a_3 \simeq 212 \text{ nm} \quad (14)$$

Thus the ‘semi-infinite slab’ curve of Fig. 3 is the $n = 3$ curve of Fig. 2 scaled to temperature units using Eq. (11).

B. Thin Slab (without Casimir)

From far enough away any slab will appear thin. The surface-atom interaction will behave like

$$\frac{-c_3}{x^3} - \frac{-c_3}{(x+d)^3} \simeq \frac{-3dc_3}{x^4} \quad (15)$$

for $x \gg d$, where d is the thickness of the slab. The resulting c_4 coefficient equal to $3dc_3$ gives an a_4 coefficient that can be written as

$$a_4 = \sqrt{\frac{2m}{\hbar^2} 3dc_3} = a_3 \left[\frac{3d}{a_3} \right]^{(1/2)}. \quad (16)$$

For macroscopic values of $d (\gg a_3)$ then, it is only for vanishingly small incident energies that the finiteness of the slab becomes apparent. For any macroscopic d this will be physically irrelevant. For microscopic $d (\ll a_3)$ however, this window in energy over which the thinness of the slab makes an appreciable difference can be larger and even prevail for all energies. To continue our illustrative example we pick the microscopic value of $d = 10 \text{ nm}$. This makes $a_4 \simeq 800 \text{ nm}$. The ‘thin slab’ curve of Figure 3 shows that the sticking probabilities are substantially reduced and the onset of Quantum Reflection occurs at a much higher energy.

As a benchmark case, we also include what will likely be the physically limiting case for a continuous film of $d = 1 \text{ nm}$. This further reduces the sticking probabilities for a fixed temperature by a factor of $\sqrt{10}$, because the important quantity a_4 is reduced by this much. (Eq.(16)). The transition temperature appears to have increased by 3 orders of magnitude versus the semi-infinite case.

C. Semi-infinite slab (Casimir Regime)

As the incoming energy ϵ tends to 0, we have seen that the turn-around region from which the atom ‘quantum reflects’ moves progressively further away from the slab. But at large distances, however, it is well known that the interaction potential itself takes on a different form due to Casimir effects. In particular, a semi-infinite dielectric slab (dielectric constant ϵ_s) has an interaction potential with an atom of polarizability α given by

$$V_{\text{slab-atom}}(x) = \frac{-3 \hbar c \alpha}{8\pi} \frac{\epsilon_s - 1}{x^4} \frac{\epsilon_s - 1}{\epsilon_s + 37/23} \quad x \rightarrow \infty \quad (17)$$

$$= \frac{-235(eV - \text{\AA})\alpha}{x^4} \frac{\epsilon_s - 1}{\epsilon_s + 37/23} \quad x \rightarrow \infty \quad (18)$$

Even for sufficiently large x , the form above is not exact but a good approximation found in Ref. [7]. Our purpose here is only to estimate the various numbers to see their relevance. It will suffice to put $\alpha_{Ne} = 0.39 \text{\AA}^3$ and the last factor involving ϵ_s is replaced by 1 since most solids and liquids have ϵ_s substantially greater than 1. This gives a $c_4^{(C)}$ coefficient of $9 \times 10^4 \text{ meV } \text{\AA}^4$ and hence a resulting $a_4^{(C)} = 93 \text{ nm}$. The superscript ‘C’ reminds us it is due to the Casimir interaction which is valid only for large enough x .

To estimate the distance beyond which the Casimir form itself is valid, we use the statement from Ref.

[8]: ‘Within a factor of 2, the van der Waals potential is correct at distances less than $0.12\lambda_{tr}$, while the Casimir potential is correct at distances at longer range.’ $\lambda_{tr} = [1, 240 \text{ nm}](\frac{\epsilon V}{\Delta E})$ here is the wavelength associated with the transition between the ground and excited state that gives the atom its polarizability. ΔE is the transition energy. Knowing this much we may deduce the qualitative features of the sticking probability curve the arguments being similar to the cases above.

For this Casimir case and the one below, however, there is a caveat to all this. The exact manner in which the potential changes its near range form to its long-range Casimir form can certainly affect the sticking probabilities at the intermediate energy where it makes this transition. Some numerical experimentation choosing arbitrary forms of the potential having the correct short range and long-range behavior, confirms this. Therefore the curves in figure 3 involving Casimir forces are only quantitatively and *not* quantitatively correct.

D. Thin Slab (Casimir Regime)

Even for a thin slab we expect that the distance at which the Casimir interaction is valid remains the same as for a semi-infinite slab made of the same material. At these distances if $x \gg d$ is also valid, then one may expect the surface atom interaction to behave like

$$\frac{-c_4^{(C)}}{x^4} - \frac{-c_4^{(C)}}{(x+d)^4} \simeq \frac{-4dc_4^{(C)}}{x^5} \quad (19)$$

The length scale

$$a_5^{(C)} = a_4^{(C)} \left[\frac{4d}{a_4^{(C)}} \right]^{1/3} \quad (20)$$

associated with this $c_5 = 4dc_4^{(C)}$ coefficient makes $a_5^{(C)} = 717\text{nm}$. Figure 3 shows a slight decrease in the sticking probabilities, the effect being evidently less here than in the case of the thick slab.

E. Hydrogen on ‘thick’ Helium

Rather atypical, but extremely favourable parameters ($c_3 = 18 \text{ meV } \text{\AA}^3$) are found in the case of Hydrogen atoms incident on bulk liquid Helium. Evidence for quantum reflection was experimentally seen in this system. [9] A comparison with the parameters used in our example of Ne on SiN:

$$m_{\text{Ne}}/m_H = 20.03 \quad \text{and} \quad c_3^{(\text{Ne-SiN})}/c_3^{(\text{H-He})} = 220/18. \quad (21)$$

With the use of Eq. (11), we see that the sticking probabilities for this case are in fact the same curves as in Figure 3 except shifted to the right in temperature by about

6.1 orders of magnitude. This puts it exactly in the milli-Kelvin regime where sticking probabilities of about 0.01 to 0.03 were observed as temperatures ranged from about 0.3 mK to 5 mK. [9] However, the sticking probabilities predicted by the ‘semi-infinite slab^(C)’ curve of Fig. 3 are about a factor 2.5 too large, but we feel there is good reason for this. We already mentioned the qualitative manner in which the Casimir forces were included but it seems that a greater error is caused for another reason. The length scale $a_3 = 17 \text{ nm}$ for H-He is so small that the WKB error is close in (see Fig. 1) where the interaction potential is not exactly of the form $\sim 1/x^3$. Practically speaking this means that the region over which we must integrate Eq.(7) must include points close to the slab to get some convergence and thus we are violating the assumption that the potential is $\sim 1/x^3$ there. This problem would not plague the Ne-SiN case too much, because the length scale there is substantially bigger. For H-He we must include some short-range information to get an improvement. Still it is the long-range forces that are mostly responsible. Ref [10,11] and others have modeled this close range behaviour and obtained better agreement; the improvement coming from explicit consideration of the bound states supported by the close range potential. These appear in the potential matrix elements of perturbation theory.

VI. RELATION TO THRESHOLD BEHAVIOR

We now wish to take a broader view of the quantum reflection behaviour at threshold ($k \rightarrow 0$), and the sticking that sets in as the energy is increased - a Post Threshold behavior. In particular we want to make connection to, and extend the well-known threshold behaviors of inelastic rates which were first stated most generally by Wigner in Ref [12]. For example, Wigner showed that the exothermic excitation rates for collisions between two bodies with bound internal degrees of freedom tend to a constant value as their relative translational energy tends to 0, provided there is no resonance at the 0 translational energy threshold. Equivalently, the exothermic inelastic cross-section diverges as $1/v$, a fact known in the still older literature as the ‘ $1/v$ law’. v is the relative velocity of the collision. Notice especially the proviso in the statement above, that there be no resonance at the threshold energy; suggesting that the many resonances between 0 and ϵ provided by a many body target could make the law inoperative. But the entire thrust of Part 1 was to establish quite generally that this many-resonance regime was precisely the one for which the old ‘ $1/v$ law’ is reinstated.

Here we re-examine the Wigner behaviour from a different point of view using our understanding of quantum reflection. In addition to furthering an intuitive understanding of the Wigner behaviour, viewing things in this way will lead naturally to predicting a generic post

threshold behavior (e.g. the $1/v$ law is replaced by a $1/v^2$ law) and an understanding of when the sticking sets back in as ϵ is increased.

The reader will have noted that we have shifted our attention to a three dimensional geometry of incidence on a localized cluster instead of the one dimensional case of incidence on a slab. So long as the target dimensions are dwarfed by the incidence wavelength we will find that both problems are effectively one dimensional due to the fact that it is only the s-wave which can penetrate the interaction region. For clarity we will deal with both cases separately.

A. Threshold and Post-Threshold Inelastic Cross-sections

The starting point is the template provided by the golden rule

$$d\sigma_{e \rightarrow c} \propto \frac{1}{k} \rho(E_c) \left| \int_{\text{all } \vec{r}} d^3r \phi_{c, \vec{k}_c}^{(-)}(\vec{r}) U_{ce}(\vec{r}) \phi_{e, \vec{k}}^{(+)}(\vec{r}) \right|^2 \quad (22)$$

for the differential cross-section for inelastic transitions from internal state $\Omega_e(u)$ to $\Omega_c(u)$ where \vec{k} and \vec{k}_c are the incoming and outgoing directions of the incident atom. We describe briefly how Eq. (22) is arrived at.

For each internal state $\Omega_c(u)$ ($c = 1, 2, \dots, n$) that we may imagine freezing the target in (u incorporates all the target degrees of freedom), there is some effective potential felt by the incoming atom. These potentials are just the diagonal elements of the complete interaction potential $U(x, u)$ in the $\Omega_c(u)$ basis, which if present all by themselves (off-diagonal elements 0) could only cause an elastic collision to occur. It is the off-diagonal elements that may be thought of as causing the inelastic transitions. Treating them as a perturbation on the elastic scattering wavefunctions we use the Golden Rule to obtain Eq.(22). $\rho(E)$ is the energy density of states of the free atom. $\phi_{e, \vec{k}}^{(+)}(\vec{r})$ is the entrance channel wavefunction and $\phi_{c, \vec{k}_c}^{(-)}(\vec{r})$ is the final channel wavefunction. They are both exact elastic scattering wavefunctions in the potentials $U_{ee}(\vec{r})$ and $U_{cc}(\vec{r})$ respectively. The factor of $1/k$ divides the Golden Rule rate by the flux to get the probability.

Now all the k dependence of $d\sigma_{e \rightarrow c}$ and hence $\sigma_{e \rightarrow c}$ is due to

- 1) the factor $1/k$ and
- 2) The sensitive k -dependence of the amplitude of the entrance channel wavefunction inside the interaction region over which the overlap integral of Eq.(22) takes place. This is simply because the incoming amplitude is more reflected away by the potential as $k \rightarrow 0$ resulting in the interior amplitude being suppressed by a factor of k as compared to what one would expect classically.

1. Incidence on a Slab

For this one-dimensional situation we speak of an inelastic probability instead of a cross-section, but otherwise Eq.(22) remains entirely valid here also with the obvious modifications.

For $k \rightarrow 0$, when WKB is invalid, we established quite generally [2] that the entrance channel wavefunction $\phi_e(x)$ when normalized to have a fixed incoming flux, had its amplitude inside the interaction region behaving like

$$\phi_e(x_{\text{inside}}) \sim k \quad \text{Threshold} \quad (23)$$

Now the change from quantum reflection at threshold to sticking at post threshold (see Fig.2) begins to occur at those energies at which the WKB wavefunctions - which show no quantum reflection - may be increasingly trusted. At these energies where WKB is valid we may simply use the well-known WKB amplitude factor $1/\sqrt{k(x)}$, to conclude that

$$\phi_e(x_{\text{inside}}) \sim \sqrt{k} \quad \text{Post - Threshold.} \quad (24)$$

The probability density of being found inside then behaves like k^2 at threshold (quantum reflection) and like k at post threshold (no quantum reflection) respectively.

It is quite natural that the probability density inside the interaction region is smaller compared to the outside by a factor of k , even when there is no quantum reflection. This is simply a kinematical effect: where the particle is moving faster, it is less likely to be found by a factor inversely proportional to its velocity there. Classically what is unexpected is that for small enough k near threshold, the probabilities inside are *further* suppressed by a factor of k . Quantum reflection of the amplitude from the region around $|V(x)| = \epsilon$ (section II), goes hand in hand with the quantum suppression of the amplitude within this region. So finally including this k -dependence of the amplitude of $\phi_e(x)$ found in equations (23) and (24) we get

$$\begin{aligned} P_{e \rightarrow c} &\propto k && \text{Threshold} \\ P_{e \rightarrow c} &\propto \text{const.} && \text{Post - Threshold} \end{aligned} \quad (25)$$

2. Incidence on a cluster

Since for large wavelengths only the s-wave interacts with the cluster it is clear that the problem may be reduced in the usual manner to a one dimensional problem again. Therefore for a unit *s-wave flux* the inelastic probabilities will behave as before as in equations (25), but what is really relevant is a unit *plain wave* flux which provides a s-wave flux of π/k^2 . i.e. Even though the problem is one-dimensional in the radial co-ordinate, the required normalization for the incoming flux is not fixed

to be a constant as before, but is now required to grow as $\sim 1/k^2$, in order to correctly account for the increasing (as $k \rightarrow 0$) range of impact parameters that all ‘count as’ s-wave. Thus we have simply to multiply the one-dimensional probabilities of equations (25) by this factor of $1/k^2$, and conclude that the inelastic cross-sections for this cluster geometry behave like

$$\begin{aligned} \sigma_{e \rightarrow c} &\propto \frac{1}{k} && \text{Threshold} \\ \sigma_{e \rightarrow c} &\propto \frac{1}{k^2} && \text{Post – Threshold} \end{aligned} \quad (26)$$

The Threshold result of Eq. (26) is just the Wigner ‘ $1/v$ law’ we spoke of in section VI. But now we can say more. As the incoming wavelength λ increases, we first witness for large enough λ a quadratic dependence to the exothermic cross-section ($\sigma \propto \lambda^2$). It is only at still larger wavelengths that this dependence eventually changes over to a linear one ($\sigma \propto \lambda$). This happens when the sticking yields to the quantum reflection. This energy is mostly determined by the long range form of the potential, and has nothing to do with the bound state energies or any other details involving the interaction potential.

VII. CONCLUSION

Examining the WKB error term provided a quick and easy way to estimate the threshold temperatures required to observe quantum reflection. It became transparent that only power laws dying faster than $-1/x^2$ were capable of acting as quantum reflectors. The validity of WKB at higher temperatures heralded a post-threshold behavior in which the atom sticks. Even for other geometries such as incidence on a localised three dimensional cluster, a WKB analysis together with the Fermi Golden Rule provided a simple understanding of this threshold and post-threshold behavior in terms of inelastic processes being shut off due to a reflection of the incoming amplitude. The extremely long incoming wavelength is invariably impedance mismatched (for potentials shorter ranged than $1/r^2$) by the abrupt change of wavelength in the interaction region, and is therefore reflected. It should be clear that even a repulsive interaction will obviously provide such a mismatch so that the Wigner behavior, or quantum reflection, is quite general; though of course most dramatic if the potential is attractive as we have been considering throughout.

This effect of quantum reflection/suppression, which is ultimately responsible for the threshold behaviour, is dynamical in that it is caused by the presence of the interaction potential. We feel that the original derivation by Wigner that focuses on the $k \rightarrow 0$ behaviour of the free space wave functions tends to obscure this physical origin of threshold behaviour. The golden rule approach makes it more explicit and especially paves the way for predicting the Post-Threshold behaviour.

ACKNOWLEDGMENTS

A.M. is most grateful to Michael Haggerty for his kind help and advice and for always being available to discuss things with. A.M. thanks Alex Barnett for pointing him to the references on the Casimir interactions.

This work was supported by the National Science Foundation through a grant for the Institute for Theoretical Atomic and Molecular Physics at Harvard University and Smithsonian Astrophysical Observatory; National Science Foundation Award Number CHE-0073544.

This work was also supported by the National Science Foundation by grants PHY-0071311 and PHY-9876927.

-
- [1] paper1
 - [2] We gave the heuristic elementary reason for the suppressed behaviour of Eq. (23) in Sec III of paper I, where we then attempted to rigorously justify it.
 - [3] J. E. Lennard-Jones *et. al.*, *Proc. R. Soc. London*, Ser. A **156** 6, (1936); Ser. A **156** 36, (1936).
 - [4] G. Vidali, G. Ihm, Hye-Young Kim, and Milton Cole, *Surface Science Reports* **12**, 133-181 (1991)
 - [5] R. E. Grisenti, W. Schoelkopf, J. P. Toennies, G. C. Hegerfeldt, and T. Khler *Phys. Rev. Lett.* **83**, 1755 (1999)
 - [6] R. Cote *et. al.* *Phys. Rev. A* **56**, 1781 (1997)
 - [7] L. Spruch, Y. Tikochinsky *Phys. Rev. A* **48**, 4213 (1997)
 - [8] E.A. Hinds V. Sandoghdar, *Phys. Rev. A* **43**, 398 (1991) in particular section II.
 - [9] Ite A. Yu, John M. Doyle, *et. al.* *Physical Review Letters* Vol. 71(10), 1589 (September 1993).
 - [10] C. Carraro and M. Cole *Physical Review B*. Vol. 45(22), 1589 (June 1992).
 - [11] T.W. Hijmans and J.T.M. Walraven and G.V. Shlyapnikov *Physical Review B*. Vol. 45(5), 2561 (February 1992).
 - [12] E. P. Wigner, *Physical Review*, Vol. 73, 1002 (1948)